

1 Assessing the microbial bioavailability and rate constants of dissolved organic matter by
2 fluorescence spectroscopy in the coastal upwelling system of the Ría de Vigo

3

4 Christian Lønborg ^{a,b}, Xosé A. Álvarez-Salgado ^a, Keith Davidson ^b, Sandra Martínez-
5 García ^c and Eva Teira ^c

6

7 ^a CSIC, Insituto de Investigacións Mariñas, Eduardo Cabello 6, 36208 Vigo, Spain

8 ^b Scottish Association for Marine Science, Oban, Argyll, PA37 1QA, United Kingdom

9 ^c Departamento de Ecoloxía e Bioloxía Animal, Universidade de Vigo, 36200 Vigo, Spain

10

11 *Corresponding author:

12 Tel. +34 986 231 930

13 Fax. +34 986 292 762

14 Email: clonborg@gmail.com

15 **Abstract**

16 The time course of colored dissolved organic matter (CDOM) absorption and
17 fluorescence were monitored during 50 to 70 days of laboratory incubations with water
18 collected in the coastal upwelling system of the Ría de Vigo (NW Iberian Peninsula) under
19 contrasting hydrographic conditions. CDOM fluorescence at peak-T (Ex/Em, 280/350 nm),
20 characteristic of protein-like materials, decayed at a 1st order rate constant (k_T) of $0.28 \pm$
21 0.13 day^{-1} (average \pm SD). k_T covaried ($R^2 = 0.86$, $p < 0.0002$) with the rate constant of the
22 bulk DOC (k_{DOC}), but the protein-like materials degraded $72 \pm 23\%$ faster than DOC.
23 Therefore, this study confirms that the CDOM fluorescence at peak-T can be used as a
24 proxy to a DOM fraction significantly more labile than the bulk bioavailable DOC. In
25 parallel with the decay of DOC and protein-like fluorescence, an increase in CDOM
26 fluorescence at peak-M (Ex/Em, 320/410 nm) during the course of the incubations verified
27 the production of marine humic-like substances as a by product of the microbial
28 metabolism. CDOM fluorescence at peak-M built up at a production rate (k_M) of $0.06 \pm$
29 0.01 day^{-1} (average \pm SD) in the Ría de Vigo. Furthermore, the slope of the linear
30 regression between k_{DOC} and k_M ($R^2 = 0.64$, $p < 0.001$) revealed that the formation of marine
31 humic-like substances occurred at about one fifth of the rate of net DOC consumption.

32

33 Keywords: DOC, bioavailable, refractory, rate constant, fluorescence spectroscopy

34 **1. Introduction**

35 Dissolved organic carbon (DOC) is the major form of organic carbon in aquatic
36 environments playing a key role in global biogeochemical cycles (Carlson 2002). DOC is a
37 heterogeneous pool of molecules resulting from multiple biotic processes of both
38 autochthonous and allochthonous origin (Scully et al. 2004). Most of the DOC pool is
39 refractory to microbial degradation over time-scales of years but a variable fraction can be
40 used by micro-organisms (e.g. Lønborg and Søndergaard 2009), with autochthonous DOC
41 considered more bioavailable than allochthonous DOC (Cauwet 2002).

42 Fluorescence spectroscopy has been applied to study dissolved organic matter
43 (DOM) dynamics, as the fluorescence intensity depend on the concentration but also on the
44 chemical composition of DOM (Coble et al. 1990). Earlier studies have given information
45 about the main DOM fluorophores: protein- and humic-like compounds (Coble et al. 1990;
46 Stedmon and Markager 2005). Protein-like fluorescence, associated with the aromatic
47 amino acids (tyrosine, tryptophan and phenylalanine), has been suggested as indicators of
48 the dynamics of total hydrolyzable amino acids, THAA (Yamashita and Tanoue 2003). The
49 THAA pool is considered bioavailable and can contribute substantially to the bacterial
50 carbon and nitrogen demand in marine systems (Coffin 1989). In addition, the fluorescence
51 of humic-like compounds has been suggested as a suitable proxy for refractory DOM, but
52 has also been identified as a by-product of in situ microbial degradation processes (Nieto-
53 Cid et al. 2006; Yamashita and Tanoue 2008). These studies suggest that the protein- and
54 humic-like fluorescence could be used to study labile and refractory DOM in the marine
55 environment. However, quantitative relationships between these variables are still lacking.

56 The coastal upwelling area of the Ría de Vigo (NW Iberian Peninsula) produces and
57 processes large amounts of DOC (Álvarez-Salgado et al. 2001), and is therefore an

58 appropriate area to establish if a quantitative relationship between fluorescence
59 spectroscopy measurements and the bioavailability and rate constant of DOC exists.
60 Complementing the study by Lønborg et al. (2009b) on the kinetics and C: N: P molar
61 ratios of DOM degradation in the Ría de Vigo, we show here new insights on the dynamics
62 of the consumption of labile and the production of refractory DOM based on fluorescence
63 spectroscopy measurements during the course of the same experiments.

64

65 **2. Material and methods**

66 *2.1 .Study area and sampling program*

67 The Ría de Vigo is a large (3.32 Km³) coastal embayment on the NW Iberian
68 Peninsula influenced by wind-driven upwelling and downwelling periods. Upwelling
69 favourable northerly winds dominate from April to October bringing cold and nutrient-rich
70 water into the ría. Southerly winds dominate the rest of the year, resulting in downwelling
71 forcing warm and nutrient-poor shelf surface water into the embayment (Álvarez-Salgado
72 et al. 2003). Fig. 1 shows the study site, which was near the main channel in the middle
73 section of the embayment. Samples from this location are influenced by both continental
74 and oceanic contributions and have proved to be representative of the processes occurring
75 in the embayment (Nogueira et al. 1997).

76 As described in Lønborg et al. (2009b), water for the laboratory incubation
77 experiments was collected in autumn (20 and 27 September, and 4 October 2007), winter
78 (31 January, 7 and 14 February 2008), spring (17 and 24 April 2008), and summer (26
79 June, 3 and 7 July 2008) with a 25 L Niskin bottle at 5 meters depth, and combined into a
80 50 L acid washed container. Salinity and temperature profiles were recorded prior to water

81 collection with an SBE 9/11 CTD probe. Aliquots of the 50L container were taken for
82 chlorophyll *a* (Chl *a*) and inorganic nutrients determination. For Chl *a* between 100 and
83 200 mL of the water samples were filtered through a GF/F filter, which were frozen (-
84 20°C) until analysis with a Turner Designs 10000R fluorometer after 90% acetone
85 extraction (Yentsch and Menzel, 1963). Water samples for dissolved inorganic nitrogen
86 (DIN; NH₄, NO₂⁻, and NO₃⁻) and phosphate (DIP; HPO₄⁻²) were collected in 50 mL acid
87 washed (HCl) polyethylene bottles and kept frozen (-20°C) until determination with an
88 Alpkem segmented flow autoanalyser.

89 Daily offshore Ekman transport values ($-Q_x$, m² s⁻¹) were calculated according to
90 Wooster et al. (1976) from average daily geostrophic winds estimated from atmospheric
91 surface pressure charts provided at 6 h intervals by the Spanish “Instituto Nacional de
92 Meteorología”. Positive values of $-Q_x$ indicate upwelling and negative values downwelling.
93 Lønborg et al. (2009b) estimated the renewal time of the embayment from $-Q_x$ as:

94
$$t = \frac{n}{\sum_i^n |Q_{x_i}|} \cdot \frac{V}{L} \quad (1)$$

95 Where $|Q_{x_i}|$ is the absolute value of the daily offshore Ekman transport, a rough estimate of
96 the volume of water upwelled/downwelled per kilometre of coast, V is the volume of the
97 embayment from the inner reaches to the sampling site (0.53×10^9 m³) and L (2.50×10^3
98 m) is the length of the open end of the embayment at the sampling site, a 7 days running-
99 mean of $|Q_{x_i}|$ centred on the sampling date was used ($n = 7$) (see Fig. 1). The 7 days
100 running-mean was chosen as previous studies have shown that the average flushing time of
101 the Ría de Vigo is about 1 week (e.g. Alvarez-Salgado et al. 2001).

102

103 2.2. *Incubation experiments*

104 Filtration of the sample water started within 10 min of collection; one part was
105 filtered through a dual-stage (0.8 μm and 0.2 μm) filter cartridge (Pall-Acropak supor
106 Membrane) which had been pre-washed with 10 L of Milli-Q water; the second part was
107 filtered through pre-combusted (450°C for 4 h) GF/C filters to establish a microbial culture.
108 After filtration, the water was kept in the dark until arrival in the base laboratory, within 2 h
109 of collection. The water was transferred into a 20 L carboy and the microbial inoculum was
110 added to the 0.2 μm filtrate corresponding to 10% of the total volume. Water was then
111 siphoned from the carboys into calibrated 110 mL biological oxygen demand (BOD) glass
112 bottles, which were filled and allowed to overflow and then capped with ground-glass
113 stoppers. Four replicate bottles were fixed with Winkler reagents immediately after filling
114 for initial O_2 concentrations, while 4 other bottles were incubated at 15°C and fixed after 53
115 or 70 days (summer experiments only). The remaining water was transferred into 24 glass
116 500 mL glass bottles (headspace \sim 100 ml), four replicate bottles being analyzed for each
117 sub-sampling at day 0, 4, 12 and 53 or 70. Additional sub-samples for DOM fluorescence
118 measurements were taken at days 1 and 2. Incubators were kept in the dark, at 15°C. All
119 glassware used in the experiments was acid washed and then rinsed with Milli-Q water
120 prior to use.

121 After fixation, four replicated dissolved oxygen (O_2) samples were kept in the dark
122 until analyzed 24 h later by Winkler potentiometric end-point titration using a Titrino 720
123 analyzer (Metrohm). The total BOD was calculated as the difference between the initial and
124 final O_2 concentrations (in $\mu\text{mol L}^{-1}$). Since the initial and final concentrations of NH_4^+ ,
125 NO_2^- and NO_3^- were different because of nitrification during the course of the incubations

126 (data not shown), oxygen concentrations were referred to the oxidation state of nitrate: O_2c
127 $= O_2 - 0.5 \cdot NO_2^- - 2 \cdot NH_4^+$.

128 Bacterial production (BP) was determined at day 0, 4, 12 and 53 or 70 by [3H]
129 thymidine (Tdr) incorporation (Fuhrman and Azam 1980). 100 μ l of an aqueous stock
130 solution of [3H - methyl] thymidine (46 Ci mmol) was added to 9.9 mL of sample and the
131 contents were mixed. Four bottles were left and two received 10 mL trichloroacetic acid
132 (TCA) to serve as a killed control. All samples were incubated in the dark at 15°C for 2 h;
133 after which 10 mL of ice-cold TCA was added to extract the soluble thymidine pools from
134 the cells. Samples were filtered onto 0.2 μ m polycarbonate filters (pre-soaked in thymidine)
135 and washed with 95% ethanol and autoclaved Milli-Q water. Filters were then placed in
136 scintillation vials, dried at room temperature for 24 h and mixed with 10 mL of scintillation
137 fluid (Sigma-Flour). Radioactivity was measured using a spectral liquid scintillation
138 counter, with the efficiency of counting determined by the external standard method. The
139 conversion factors 2×10^{18} cells mol $^{-1}$ thymidine (Smits and Riemann 1988) and 30 fg C
140 cell $^{-1}$ (Fukuda et al. 1998) were used to convert thymidine incorporation rates into bacterial
141 carbon production.

142 Samples for analyses of the dissolved phase were collected from each of the 4
143 replicate incubation bottles by filtration through 0.2 μ m filters (Pall, Supor membrane Disc
144 Filter) to follow dissolved organic carbon (DOC) and the optical properties of colored
145 dissolved organic matter (CDOM): absorption and fluorescence. Sub-samples (10 mL) for
146 DOC analysis were collected in pre-combusted (450°C, 12 hours) glass ampoules at day 0,
147 4, 12 and 53 or 70 of the incubations and preserved by adding 50 μ L 25 % H_3PO_4 . DOC
148 sub-samples were analyzed in four replicates using a Shimadzu TOC-CSV organic carbon
149 analyzer. Three to five injections of 150 μ L were performed per replicate. Concentrations

150 were determined by subtracting a Milli-Q blank and dividing by the slope of a daily
151 standard curve made from potassium hydrogen phthalate. To avoid the small error
152 associated with day-to-day instrument variability, all samples from a given experiment
153 were analyzed on a single day. All samples were checked against deep Sargasso Sea
154 reference water (2,600 m). The deep sea reference gave an average (\pm SD) concentration of
155 $46.0 \pm 2.0 \mu\text{mol L}^{-1}$ with the nominal value for DOC provided (D.A. Hansell's laboratory)
156 being $44.0 \pm 1.5 \mu\text{mol L}^{-1}$.

157 The CDOM absorption was measured in four replicates on a Beckman Coulter DU
158 800 spectrophotometer using Milli-Q water as a blank. Before analysis samples were
159 warmed to room temperature. The absorption was measured at a wavelength of 350 nm
160 using a 10 cm quartz cuvette. The absorption coefficient (a_λ) was calculated as:

$$161 \quad a_\lambda = \frac{2.303 \cdot A_\lambda}{L} \quad (2)$$

162 Where A_λ is the optical density measured at 350 nm (m^{-1}) corrected for background
163 absorption measured at 700 nm, the factor 2.303 converts from base 10 to base e logarithms
164 and the denominator L is the cell path-length in meters (Stedmon and Markager 2001).

165 The CDOM fluorescence was measured in four replicates on a Perkin Elmer LS 55
166 luminescence spectrophotometer equipped with a xenon discharge lamp, equivalent to 20
167 kW for 8 μs duration. The detector was a red-sensitive R928 photomultiplier, and the
168 photodiode works as a reference detector. Measurements were performed at a constant
169 temperature of 20°C in a 1 cm quartz fluorescence cell. Milli-Q water was used as a
170 reference, and the intensity of the Raman peak was checked daily. Excitation/emission
171 (Ex/Em) measurements were performed at peak-T (aromatic amino acids, average Ex/Em,
172 280/350 nm; termed FDOMt), peak-A (general humic compounds, average Ex/Em 250/435

173 nm; termed FDOMa), peak-C (terrestrial humic substances, average Ex/Em = 340/440 nm;
174 termed FDOMc) and peak-M (marine humic substances, average Ex/Em 320/410 nm;
175 termed FDOMm), obtained from Coble et al. (1990). Fluorescence measurements were
176 expressed in quinine sulphate units (QSU), i.e. in $\mu\text{g eq QS L}^{-1}$, by calibrating the LS 55
177 Perkin Elmer at Ex/Em: 350 nm/450 nm against a quinine sulphate dihydrate (QS) standard
178 dissolved in 0.05 mol L^{-1} sulphuric acid.

179 Linear regression analyses were performed using the best-fit between the two
180 variables X and Y obtained by model II regression as described in Sokal and Rohlf (1995).
181 Prior to the regressions, normality was checked and the confidence level was set at 95%,
182 with all statistical analysis conducted in Statistica 6.0.

183

184 **3. Results**

185 *3.1. Seasonal and short-time scale hydrographic variability during the survey periods*

186 Lønborg et al. (2009b) have shown that the values of $-Q_x$ in Table 1 indicate a
187 transition from strong upwelling-favorable to moderate downwelling-favorable winds
188 during the autumn surveys. In winter, the embayment evolved from wind relaxation to
189 strong downwelling-favorable winds. The spring surveys occurred under moderate
190 downwelling-favorable winds, whereas initial strong upwelling-favorable winds were
191 followed by moderate downwelling during the summer surveys. Therefore, apart from the
192 seasonal variability, the range of hydrographic conditions that occur in the Ría de Vigo in
193 association with the highly variable wind regime has been sampled. In order to estimate the
194 efficiency of the ría as a DOM digester, flushing times were calculated from $-Q_x$ (see

195 section 2.1). An average value of 7 days was obtained, ranging from 3 days when coastal
196 winds were strong to 18 days for surveys that coincided with calm winds (Table 1).

197 As indicated above, the combination of the seasonal cycle and the short-time scale
198 variability imposed by coastal winds create contrasting hydrographic conditions at the
199 sampling site. During the autumn surveys surface (5 m) temperature decreased from $> 16^{\circ}\text{C}$
200 on 20-Sep-2007 to $< 14^{\circ}\text{C}$ during the following two weeks. Concomitantly, DIN increased
201 from 3 to $13 \mu\text{mol L}^{-1}$ and Chl *a* was constant at around 3 mg m^{-3} . During the winter
202 surveys, surface temperatures were the lowest, between 13.0 and 13.5°C , Chl *a* levels were
203 $< 1.5 \text{ mg m}^{-3}$ and DIN concentration was maintained above $8 \mu\text{mol L}^{-1}$. During the spring
204 surveys, salinities were relatively low because of intense precipitation during April (153.7
205 mm from 01-Apr-2008 to 24-Apr-2008 recorded in the terrace of the host laboratory).
206 Salinity on the 24-Apr-2008 was as low as 25, coinciding with the highest chlorophyll
207 levels, $> 8 \text{ mg m}^{-3}$, and relatively low phosphate, $< 0.1 \mu\text{mol L}^{-1}$. Conversely, DIN levels
208 were $> 5 \mu\text{mol L}^{-1}$, because of the high N: P molar ratio in the nutrient salts transported by
209 the continental waters. Finally, during the summer surveys, the highest temperatures, $>$
210 17°C , and low DIN levels, $< 3 \mu\text{mol L}^{-1}$, were recorded with Chl *a* concentrations ranging
211 from 1.1 to 4.5 mg m^{-3} .

212

213 *3.2. CDOM dynamics during the course of the incubations*

214 Earlier studies have found that the microbial degradation of DOC can be limited by
215 inorganic nutrients (Del Giorgio and Davies 2003). The low DIN:DIP ratio typical of the
216 Ría de Vigo (Nogueira et al. 1997) suggests that nitrogen rather than phosphorus was likely
217 to limit DOC uptake. To test for nutrient limitation additional incubations were conducted
218 each sampling date enriched with carbon (glucose) and nitrate (data not shown). These

219 experiments showed no effect on DOC degradation, suggesting that the microbial
220 community in the incubations did not experienced nitrogen limitation.

221 The concentration of DOC decayed exponentially during the course of all the
222 incubations performed in this study (Fig. 2). Lønborg et al (2009b) adjusted the kinetics of
223 DOC utilization to a first-order exponential decay function using the Marquardt-Levenberg
224 algorithm taking the refractory pool into account:

$$225 \text{ DOC}(t) = \text{BDOC} \cdot \exp(-k_{\text{DOC}} \cdot t) + \text{RDOC} \quad (3)$$

226 Where $\text{DOC}(t)$ is the concentration of DOC at time t (0, 4, 10 and 50 or 70 days),
227 BDOC the bioavailable pool ($\mu\text{mol L}^{-1}$), k_{DOC} the rate constant (day^{-1}), t the time (days)
228 and RDOC the residual pool at the end of the incubations ($\mu\text{mol L}^{-1}$). BDOC is defined as
229 $\text{BDOC} = \text{DOC}(0) - \text{RDOC}$, where $\text{DOC}(0)$ is the initial DOC concentration. Therefore,
230 k_{DOC} was the only parameter to be adjusted.

231 $\text{DOC}(0)$, BDOC, RDOC and k_{DOC} values are reported in Table 2a. Initial DOC varied
232 between 73 and 94 $\mu\text{mol L}^{-1}$, $17 \pm 6\%$ (average \pm SD) of which was bioavailable with an
233 average half-life time, $\ln 2/k_{\text{DOC}}$, of 3.3 ± 0.9 days (average \pm SD). As reported by Lønborg
234 et al. (2009b) (i) the initial concentrations are within the values previously reported for the
235 surface layer of the Ría de Vigo; (ii) the bioavailable fraction is comparable with the values
236 found in other coastal waters, $22 \pm 13\%$, and within the range previously suggested for this
237 ecosystem, 10-30%; (iii) the k_{DOC} values are higher than in other coastal waters but
238 resembled the rates found on George Bank; and (iv) the refractory pool, $67 \pm 4 \mu\text{mol L}^{-1}$
239 (average \pm SD), is not significantly different from the DOC concentration reported for the
240 Eastern North Atlantic Central water found in the bottom layer of the ría during upwelling
241 events.

242 As for the case of DOC, the protein-like fluorescence decayed exponentially (Fig. 2)
243 and could be modelled by:

$$244 \quad \text{FDOMt}(t) = \text{BFDOMt} \cdot \exp(-k_T \cdot t) + \text{RFDOMt} \quad (4)$$

245 Where $\text{FDOMt}(t)$ is the protein-like fluorescence (QSU) at incubation time t (0, 1, 2,
246 4, 10 and 50 or 70 days), $\text{BFDOMt}(t)$ is the bioavailable FDOMt (QSU), k_T the rate constant
247 (day^{-1}), t the time (days) and RFDOMt the remaining pool at the end of the incubations. We
248 assumed that RFDOMt was constant throughout the incubations.

249 The parameters of the equations that describe the 1st order decay of protein-like
250 substances are summarized in Table 2b. A decrease of 0.55 ± 0.22 QSU (average \pm SD)
251 was observed during the course of the incubations, which indicates that $28 \pm 7\%$ of the
252 initial protein-like fluorescence is bioavailable. This bioavailable fraction decayed at a rate
253 of $0.28 \pm 0.13 \text{ day}^{-1}$ (average \pm SD) that represents a half-life time of 3.0 ± 1.3 days. It is
254 worth noting that, despite the lability of the protein-like substances, a residual signal of
255 1.35 ± 0.13 QSU (average \pm SD) remains at the end of the incubation time.

256 In parallel with the decay of DOC and FDOMt , an increase in marine humic-like
257 fluorescence of 0.56 ± 0.18 QSU (average \pm SD) was observed during the course of the
258 incubations (Fig. 2), which can be modelled by:

$$259 \quad \text{FDOMm}(t) = \text{PFDOMm} \cdot [1 - \exp(-k_M \cdot t)] + \text{FDOMm}(0) \quad (5)$$

260 Where $\text{FDOMm}(t)$ is the marine humic-like fluorescence (QSU) at incubation time t
261 (0, 1, 2, 4, 10 and 50 or 70 days), PFDOMm is the amount of FDOMm produced (QSU), k_M
262 the formation rate (day^{-1}), t the time (days) and $\text{FDOMm}(0)$ the initial FDOMm pool. Using
263 this formula it is assumed that the initial FDOMm was refractory.

264 Equation parameters summarized in Table 2c show that initial FDOMm values ranged
265 from 1.2 to 2.8 QSU and that the exponential model used to describe the FDOMm built up,
266 gave production rates (k_M) between 0.04 and 0.08 day⁻¹.

267 BFDOMt and PFDOMm are both significantly correlated with BDOC (eq 1 & 2 of
268 Table 3) and their corresponding rates, k_T and k_M are significantly correlated with k_{DOC}
269 (Fig. 3). These results indicate that (i) fluorescence spectroscopy, specifically the protein-
270 like fluorescence, can be used to follow the kinetics of degradation of bioavailable DOC;
271 (ii) fluorescent humic-like substances are a by-product of the degradation of bioavailable
272 DOC; (iii) the significant origin intercept of the relationship between k_T and k_{DOC} indicates
273 that there is a fraction of bioavailable DOC that does not cycle with bioavailable FDOMt
274 and the regression slope lower than 1 suggests that bioavailable DOC cycles slower than
275 bioavailable FDOMt; and (iv) for the case of the relationship between k_{DOC} and k_M (Fig.
276 3b), the significant origin intercept indicates the bioavailable DOC is not the only source of
277 humic-like fluorescence and the regression slope suggests that PFDOMm built-up is much
278 slower than BFDOMt decay.

279 Contrary to the changes observed in FDOMt and FDOMm, the CDOM absorption
280 coefficient at 350nm (a_{350}), did not change significantly during the course of the
281 incubations (data not shown).

282 Apart from DOC and the CDOM absorption and fluorescence,, bacterial production
283 and dissolved oxygen changes were also monitored during the course of the incubations.
284 Initial bacterial production rates (BP) ranged from 0.3 to 2.0 $\mu\text{g C L}^{-1} \text{ day}^{-1}$. Maximum
285 values were recorded in autumn and summer. BP decreased exponentially in parallel to the
286 decay of DOC and FDOMt, reaching values not significantly different from zero at the end
287 of the incubations (Fig. 2; Table 2d). The oxygen demand during the course of the 50 to 70

288 days of incubation (BOD) was converted to organic carbon consumption units using the
289 theoretical $R_C = -O_2:C_{org}$ stoichiometric molar ratios obtained by Lønborg et al. (2009b)
290 for the same experiments (Table 2e). Within the errors of estimation of BDOC, BOD and
291 R_C ($\pm 0.15 \text{ mol O}_2 \text{ mol C}^{-1}$), it can be stated that the bacterial degradation of BDOC is
292 behind the observed dissolved oxygen consumption.

293

294 **4. Discussion**

295 Differences in the initial CDOM absorption and fluorescence point to temporal
296 changes in the DOM chemical composition of the water we collected to perform the
297 incubation experiments (Nieto-Cid et al. 2005; 2006). On the one hand, protein-like
298 fluorescence has been suggested as a useful indicator of the presence of THAA, which
299 potentially could be used to trace the dynamics of labile DOM (Yamashita and Tanoue
300 2003; Stedmon and Markager 2005, Nieto-Cid et al. 2006). In this sense, significant linear
301 relationships have been found in this study between the initial protein-like fluorescence,
302 $FDOM_t(0)$, the bioavailable DOC and k_{DOC} (eq 3-4 of Table 3), suggesting that the key
303 parameters that define the bioavailability and rate constants of DOC can be derived directly
304 from the initial protein-like fluorescence of the Ría de Vigo. It is also remarkable the
305 significant positive linear relationship between the initial $FDOM_t$ and its decomposition
306 rate, k_T (eq 5 of Table 3), demonstrating that higher $FDOM_t$ concentrations would lead to
307 faster mineralization rates as observed for the case of DOC in the Ría de Vigo (Lønborg et
308 al. 2009b) and in other coastal systems (Hopkinson et al. 1997, Lønborg et al. 2009a).

309 On the other hand, the humic-like fluorescence has been used to trace the presence of
310 both allochthonous and autochthonous refractory DOM (Yamashita and Tanoue 2004; Nieto-
311 Cid et al. 2005; 2006; Yamashita and Tanoue 2008). In agreement with this, the initial

312 fluorescence of the humic-like fluorophores correlated significantly with the refractory
313 DOC (eq 6-8 of Table 3). The origin intercepts of these relationships indicated that a large
314 fraction of RDOC (52-56 $\mu\text{mol L}^{-1}$) was non-colored material. FDOMa and FDOMc were
315 inversely correlated with salinity (eq 9-10 of Table 3), and remained constant throughout
316 the incubation time (data not shown), suggesting a predominantly allochthonous refractory
317 nature for these fluorophores (Yamashita et al. 2008). Furthermore, the initial absorption
318 coefficient at 350 nm correlated significantly with the initial fluorescence of the humic-like
319 fluorophores and with the refractory DOC (eq 11-14 of Table 3), suggesting that CDOM
320 absorption could be used to trace the refractory humic substances in the water collected to
321 perform the incubation experiments (Stedmon and Markager 2001). Conversely, during the
322 course of the experiments, the observed increase in FDOMm is not accompanied by a
323 significant increase in a_{350} . This result suggests that the humic substances produced by the
324 incubated microbial cultures differ from those present in the initial waters. Note that apart
325 from possible allochthonous sources, the whole community of organisms could have
326 contributed to the production of humic substances in the initial waters.

327 The significant correlation of the initial bacterial production with the bioavailable
328 DOC (eq 15 of Table 3), together with the parallel evolution of BP and DOC during the
329 course of the incubations (Fig. 2), suggest that the inoculated natural bacterial assemblages
330 were growing only when bioavailable DOC was present in the incubated water. Therefore,
331 it confirms that the observed DOC decay was due to bacterial utilization. Furthermore, the
332 balance between the concentration of bioavailable DOC and the oxygen consumption after
333 50 to 70 days of incubation when the stoichiometric molar ratio R_C is considered (Table 2e)
334 suggest that BDOC is essentially respired by bacteria.

335 The slope of the correlation between k_T and k_{DOC} (Fig. 3a) indicated that the
336 bioavailable fraction of DOC is consumed at a rate corresponding to only $58 \pm 8\%$ of the
337 bioavailable FDOMt, i.e. that BFDOMt cycled $72 \pm 23\%$ faster than BDOC, agreeing with
338 a preferential mineralization of nitrogen over carbon-rich compounds as found in other
339 studies (Garber 1984; Hopkinson et al. 1997; 2002). The origin intercept of this correlation
340 ($0.05 \pm 0.02 \text{ day}^{-1}$) represents the average rate constant of BDOC not coupled to the
341 consumption of protein-like substances. Therefore, k_{DOC} can be viewed as the combination
342 of a basal rate constant of $0.05 \pm 0.02 \text{ day}^{-1}$ plus a rate constant corresponding to k_T linked
343 to the consumption of the labile protein-like compounds. It should be noted that the
344 observed relationship between k_{DOC} and k_T in Fig. 3a is specific for the coastal upwelling
345 area of the Ría de Vigo. This experimental approach therefore has to be repeated in any
346 other area of interest to establish the relationship between the two rate constants and,
347 therefore, to differentiate between the very labile and labile fraction in that area.

348 It has been suggested that coastal upwelling systems export labile DOC to the
349 adjacent ocean (Hansell and Carlson 1998; Álvarez-Salgado et al. 2001). Using the rate
350 constants of Table 2b and the average flushing times of water of Table 1, it results that $80 \pm$
351 13% (average \pm SD) of the BFDOMt was consumed within the embayment. Therefore, $20 \pm$
352 13% of the BFDOMt produced in the Ría de Vigo was exported to the adjacent shelf, i.e.
353 this embayment exports horizontally a significant fraction of labile organic matter.

354 The RFDOMt pool, which represents as much as $72 \pm 7\%$ of the initial FDOMt,
355 could have two likely causes: i) a large fraction of the protein-like fluorophores are of a
356 refractory nature and, therefore, FDOMt fluorescence does not only trace labile material;
357 and ii) the high FDOMt levels at the end of the incubations are caused by interference of
358 the tails of the humic-like fluorophores on the FDOMt peak. The last suggestion is

359 supported by the significant linear relationships of RFDOMm, FDOMa(0) and FDOMc(0)
360 with RFDOMt (eq 16-18 of Table 3).

361 The production of marine humic-like substances during the course of the incubations
362 further confirms that they are a by product of microbial degradation processes (Yamashita
363 and Tanoue 2004; Nieto-Cid et al. 2006). The slope of the significant ($p < 0.01$) linear
364 correlation between k_{DOC} and k_{M} (Fig. 3b), showed that humic like materials were produced
365 at a rate corresponding to $17 \pm 4\%$ of k_{DOC} . The significant origin intercept of this linear
366 regression ($0.02 \pm 0.01 \text{ day}^{-1}$) further demonstrated that DOC is not the only source of
367 FDOMm during degradation. Although this study has been based on dark incubation
368 experiments, it should be noted that the in situ produced marine humic-like materials are
369 very sensitive to the natural UV radiation that causes a rapid photo bleaching of the
370 FDOMm fluorescence (Nieto-Cid et al. 2006). Consequently, our results regarding the
371 dynamics of marine humic-like fluorophores are not directly applicable to field conditions.

372

373 **5. Conclusions**

374 This study is, to our knowledge, the first to show quantitative relationships between
375 fluorescence of colored DOM and bioavailability of DOC. We demonstrate a positive linear
376 relationship between protein-like fluorescence and the bioavailable fraction of DOC as well
377 as its rate constants, suggesting that these key parameters can be derived directly from the
378 initial protein-like fluorescence of the Ría de Vigo. Furthermore, it has also been shown
379 that a large fraction of the protein-like fluorescence can be of a non-labile nature. The study
380 also demonstrates that the humic-like fluorescence was linearly related with the refractory
381 DOC pool and that the increase of these fluorophores during the course of dark incubations
382 as a by-product of bacterial respiration could be used as a proxy to DOM mineralization

383 processes. It is proposed that future studies should test the reliability of this approach in
384 other coastal areas, to verify the usability of fluorescence spectroscopy in characterizing
385 and assessing bioavailability of DOC in marine systems.

386 **Acknowledgement**

387 This study was funded by a fellowship to C.L from the Early stage Training site
388 ECOSUMMER (MEST-CT-2004-020501). We thank the captain, crew, and technicians of
389 R/V Mytilus and the members of the Department of Oceanography of the Instituto de
390 Investigaci3n Mariñas for the collaboration during the sampling program. Access to vessel
391 time and data presented in Table 1 were provided by the RAFTING project (Impact of the
392 mussel raft culture on the benthic-pelagic coupling in a Galician Ría, grant number:
393 CTM2007-61983/MAR). The valuable suggestions and comments by three anonymous
394 reviewers and Prof. Peter J. Ieb. Williams are gratefully acknowledged.

395

396 **References**

- 397 lvarez-Salgado, X.A., Gago, J., Miguez, B.M., Prez, F.F., 2001. Net ecosystem
398 production of dissolved organic carbon in a coastal upwelling system: the Ria de Vigo,
399 Iberian margin of the North Atlantic. *Limnol. Oceanogr.* 46, 135-147.
- 400 lvarez-Salgado, X.A., Figueiras, F.G., Prez, F.F., Groom, S., Nogueira, E., Borges, A.V.,
401 Chou, L., Castro, C.G., Moncoiff, G., Ros, A.F., Miller, A.E.J., Frankignoulle, M.,
402 Savidge, G., Wollast, R., 2003. The Portugal coastal counter current off NW Spain: new
403 insights on its biogeochemical variability. *Prog. Oceanogr.* 56, 281-321.
- 404 Carlson, C.A., 2002 Chemical Composition and Reactivity. In: Hansell, D.A., Carlson,
405 C.A. (Eds.), *Biogeochemistry of marine dissolved organic matter*. Academic Press,
406 pp. 59-90.
- 407 Cauwet, G., 2002. DOM in coastal areas. In: Hansell, D.A., Carlson, C.A. (Eds.),
408 *Biogeochemistry of marine dissolved organic matter*. Academic Press, pp. 579-609.

409 Coble, P.G., Green, S.A., Blough, N.V., Gasgolian, R.B., 1990. Characterization of
410 dissolved organic matter in the Black Sea by fluorescence spectroscopy. *Nature* 348,
411 432-435.

412 Coffin, R.B., 1989. Bacterial uptake of dissolved free and combined amino acids in
413 estuarine waters. *Limnol. Oceanogr.* 34, 531– 542.

414 Del Giorgio, P., Davies, J., 2003. Patterns of dissolved organic matter lability and
415 consumption across aquatic ecosystems. In: Findlay, S.E.G., Sinsabaugh, R.L. (Eds.),
416 *Aquatic Ecosystems: Interactivity of Dissolved Organic Matter*. Academic Press, pp.
417 399-424

418 Fuhrman, J. A., Azam, F., 1980. Bacterioplankton secondary production estimates for
419 coastal waters of British Columbia, Antarctica, and California. *Appl. Environ. Micro.*
420 36, 1085–1095.

421 Fukuda, R., Ogawa, H., Nagata, T., Koike I., 1998. Direct Determination of Carbon and
422 Nitrogen Contents of Natural Bacterial Assemblages in Marine Environments. *Appl.*
423 *Environ. Micro.* 64, 3352-3358.

424 Garber, J.H., 1984. Laboratory study of nitrogen and phosphorus remineralization during
425 the decomposition of coastal plankton and seston. *Estuar. Coast. Shelf Sci.* 18, 685 -
426 702.

427 Hansell, D.A., Carlson, C.A., 1998. Net community production of dissolved organic
428 carbon. *Global Biogeochem. Cycles.* 12, 443-453.

429 Hopkinson, C.S., Fry, B., Nolin A.L., 1997. Stoichiometry of dissolved organic matter
430 dynamics on the continental shelf of the northeastern U.S.A. *Cont. Shelf. Res.* 17,
431 473- 489.

- 432 Hopkinson, C.S., Vallino, J.J., Nolin, A.L., 2002. Decomposition of dissolved organic
433 matter from the continental margin. *Deep-Sea Res. II* 49, 4461-4478.
- 434 Lønborg, C., Søndergaard, M., 2009. Microbial availability and degradation of dissolved
435 organic carbon and nitrogen in two coastal areas. *Estuar, Coast. Shelf Sci.* 81, 513-
436 520.
- 437 Lønborg, C., Davidson K., Álvarez-Salgado X.A., Miller A.E.J., 2009a. Bioavailability and
438 bacterial degradation rates of dissolved organic matter in a temperate coastal area
439 during an annual cycle. *Marine Chemistry* 113, 219-226.
- 440 Lønborg C., Álvarez-Salgado X.A., Martínez S., Miller A.E.J., Teira E. 2009b.
441 Stoichiometry of dissolved organic matter and the kinetics of its microbial
442 degradation in a coastal upwelling system. *Aquat Microb Ecol.* Doi:
443 10.3354/ame01364.
- 444 Nieto-Cid, M., Álvarez-Salgado, X.A., Gago, J., Pérez, F.F., 2005. DOM fluorescence, a
445 tracer for biogeochemical processes in a coastal upwelling system (NW Iberian
446 Peninsula). *Mar Ecol Prog Ser.* 297, 33–50.
- 447 Nieto-Cid, M., Álvarez-Salgado, X.A., Pérez, F.F., 2006. Microbial and photochemical
448 reactivity of fluorescent dissolved organic matter in a coastal upwelling system.
449 *Limnol. Oceanogr.* 51, 1391-1400.
- 450 Nogueira, E., Pérez, F.F., Ríos, A.F., 1997. Seasonal patterns and long-term trends in an
451 estuarine upwelling ecosystem (Ría de Vigo, NW Spain). *Estuar, Coast. Shelf Sci.* 44,
452 285-300.
- 453 Scully, N.M., Maie, N., Dailey, S.K., Boyer, J.N., Jones, R.D., Jaffe R., 2004. Early
454 diagenesis of plant-derived dissolved organic matter along a wetland, mangrove,
455 estuary ecotone. *Limnol. Oceanogr.* 49, 1667-1678.

- 456 Smits, J.D., Riemann, B., 1988. Calculation of cell production from [3H] thymidine
457 incorporation with freshwater bacteria. *Appl. Environ. Micro.* 54, 2213-2219.
- 458 Sokal, F.F., Rohlf, F.J., 1995. *Biometry*. Freeman, New York.
- 459 Stedmon, C.A., Markager, S.S., 2001. The optics of chromophoric dissolved organic matter
460 (CDOM) in the Greenland sea: An algorithm for differentiation between marine and
461 terrestrially derived organic matter. *Limnol. Oceanogr.* 46, 2087-2093.
- 462 Stedmon, C.A., Markager, S.S., 2005. Tracing the production and degradation of
463 autochthonous fractions of dissolved organic matter by fluorescence analysis. *Limnol.*
464 *Oceanogr.* 50, 1415-1426.
- 465 Yamashita, Y., Tanoue, E., 2003. Chemical characterization of protein-like fluorophores in
466 DOM in relation to aromatic amino acids. *Mar. Chem.* 82, 255-271.
- 467 Yamashita, Y., Tanoue, E., 2004. In situ production of chromophoric dissolved organic
468 matter in coastal environments. *Geophys. Res. Lett.* 31, Doi:10.1029/2004GL019734.
- 469 Yamashita, Y., Tanoue, E., 2008. Production of bio-refractory fluorescent dissolved
470 organic matter in the ocean interior. *Nature Geosci.* 1, 579-582.
- 471 Yamashita, Y., Jaffé, R., Maie, N., Tanoue, E., 2008. Assessing the dynamics of dissolved
472 organic matter (DOM) in coastal environments by excitation emission matrix
473 fluorescence and parallel factor analysis (EEM-PARAFAC). *Limnol. Oceanogr.* 53,
474 1900-1908.
- 475 Yentsch, C. S., Menzel D. W., 1963. A method for the determination of phytoplankton
476 chlorophyll and phaeophytin by fluorescence, *Deep Sea Res. Oceanogr. Abstr.* 10,
477 221-231.
- 478 Wooster, W. S., Bakun, A., McClain, D. R., 1976. The seasonal upwelling cycle along the
479 eastern boundary of the North Atlantic. *J. Mar. Res.* 34, 131-141.

480 **Figure legends**

481 Fig. 1. Map showing the sampling station (filled circle) in the middle Ría de Vigo (NW
482 Iberian Peninsula).

483 Fig. 2. Time course of dissolved organic carbon (DOC), protein-like (FDOMt) and marine
484 humic-like fluorescence (FDOMm) and bacterial production during the incubations
485 conducted in (a), (b), (c),(d) autumn, (e), (f), (g), (h) winter, (i), (j), (k), (l) spring and (m),
486 (n), (o), (p) summer. Incubation start dates are shown in legends. Error bars represent
487 standard errors.

488

489 Fig 3. Plots of the linear relationship between (a) the rate constants (day^{-1}) of FDOMt (k_T)
490 and DOC (k_{DOC}); and (b) k_{DOC} and k_M . Solid lines represent the corresponding regression,
491 the dashed line in panel a is the 1:1 line and the error bars are the standard errors. $R^2 =$
492 coefficient of determination, $p =$ level of significance.

Table 1. Conditions in the Ría de Vigo at the sampling site (5 m depth) on the water collection dates. Salinity, temperature, chlorophyll *a*, dissolved inorganic phosphate (DIP) and inorganic nitrogen (DIN), and CDOM absorption coefficients (a350). Seven days running means of the offshore Ekman transport ($-Q_x$) and derived flushing times are also shown.

Date	Salinity	Temperature (°C)	Chlorophyll <i>a</i> (mg m ⁻³)	DIP (μmol L ⁻¹)	DIN (μmol L ⁻¹)	a350 (m ⁻¹)	$-Q_x$ (m ³ s ⁻¹ km ⁻¹)	Flushing time (days)
20-Sep-2007	35.5	16.2	3.26	0.19 ± 0.02	3.17 ± 0.53	0.38 ± 0.04	551	4.4
27-Sep-2007	35.6	14.1	2.81	0.68 ± 0.01	10.34 ± 0.02	0.26 ± 0.03	-82	3.7
4-Oct-2007	35.4	13.8	2.80	0.54 ± 0.03	12.66 ± 0.38	0.25 ± 0.01	-133	11.0
31-Jan-2008	35.0	13.0	1.52	0.46 ± 0.01	9.60 ± 0.21	0.23 ± 0.02	6	5.3
7-Feb-2008	34.5	13.1	0.81	0.56 ± 0.02	11.34 ± 0.24	0.31 ± 0.01	-753	3.2
14-Feb-2008	35.2	13.4	1.13	0.42 ± 0.01	8.16 ± 0.30	0.26 ± 0.01	-127	18.0
17-Apr-2008	34.8	14.3	3.04	0.09 ± 0.02	0.40 ± 0.10	0.29 ± 0.01	-147	5.5
24-Apr-2008	25.0	15.5	8.42	0.09 ± 0.01	5.25 ± 0.20	0.60 ± 0.01	-87	8.6
26-Jun-2008	35.1	17.4	4.32	0.27 ± 0.01	0.72 ± 0.25	0.37 ± 0.09	782	3.0
3-Jul-2008	35.6	17.1	1.16	0.02 ± 0.01	1.20 ± 0.16	0.32 ± 0.01	-224	5.1
10-Jul-2008	35.4	18.4	4.52	0.38 ± 0.01	3.07 ± 0.20	0.39 ± 0.01	-36	9.0

Table 2. Initial (DOC(0), FDOMt(0)) used (BDOC, BFDOMt), end (RDOC, RFDOMt) concentrations and rate constants (k_{DOC} , k_{T}) of a) dissolved organic carbon (DOC) and b) protein-like fluorescence (FDOMt). c) Shows the initial (FDOMm(0)), produced (PFDOMm) and total (RFDOMm) pools of FDOMm fluorescence and build-up rates of FDOMm (k_{M}). Table 2d) Bacterial production measured at day 0 (BP(0)) , 4 (BP(4)), 12 BP(0) and 53/70 (BP(53/70)) of the incubations. e) The initial ($\text{O}_{2\text{C}}(0)$) and final ($\text{O}_{2\text{C}}(53/70)$) oxygen concentrations and biological oxygen demand (BOD). The difference between the measured BOD and the expected BOD from the complete oxidation of BDOC ($= \text{BDOC} \cdot R_{\text{C}}$) is also shown in Table 2.e). R_{C} is the theoretical stoichiometric molar ratio of O_2 consumption to CO_2 production obtained in Lønborg et al. (2009b) from the C:N:P composition of BDOM for the same experiments. Values are averages of 4 replicates \pm standard error. R^2 = coefficient of determination.

Date	DOC(0) ($\mu\text{mol L}^{-1}$)	BDOC ($\mu\text{mol L}^{-1}$)	RDOC ($\mu\text{mol L}^{-1}$)	k_{DOC} (day^{-1})	R^2	a)
20-Sep-2007	94 \pm 1	29 \pm 3	65 \pm 1	0.35 \pm 0.04	0.99	
27-Sep-2007	79 \pm 1	15 \pm 1	62 \pm 1	0.23 \pm 0.05	0.99	
4-Oct-2007	75 \pm 2	12 \pm 2	63 \pm 1	0.18 \pm 0.03	0.98	
31-Jan-2008	75 \pm 1	9 \pm 1	67 \pm 1	0.11 \pm 0.03	0.97	
7-Feb-2008	77 \pm 1	7 \pm 1	70 \pm 1	0.11 \pm 0.01	1.00	
14-Feb-2008	73 \pm 1	10 \pm 2	63 \pm 1	0.20 \pm 0.01	0.95	
17-Apr-2008	81 \pm 1	13 \pm 1	68 \pm 1	0.20 \pm 0.02	0.99	
24-Apr-2008	85 \pm 1	11 \pm 1	73 \pm 1	0.20 \pm 0.02	0.99	
26-Jun-2008	88 \pm 1	17 \pm 2	71 \pm 2	0.30 \pm 0.08	0.94	
3-Jul-2008	82 \pm 1	14 \pm 1	68 \pm 1	0.19 \pm 0.05	0.93	
10-Jul-2008	89 \pm 2	18 \pm 1	71 \pm 1	0.30 \pm 0.05	0.98	

Date	FDOMt(0) (QSU)	BFDOMt (QSU)	RFDOMt (QSU)	k_T (day ⁻¹)	R ²	b)
20-Sep-2007	2.63 ± 0.04	1.14 ± 0.06	1.49 ± 0.02	0.60 ± 0.10	0.94	
27-Sep-2007	1.79 ± 0.05	0.52 ± 0.15	1.27 ± 0.10	0.30 ± 0.07	0.93	
4-Oct-2007	1.68 ± 0.02	0.37 ± 0.05	1.32 ± 0.04	0.22 ± 0.03	0.96	
31-Jan-2008	1.74 ± 0.03	0.43 ± 0.04	1.31 ± 0.01	0.15 ± 0.04	0.88	
7-Feb-2008	1.74 ± 0.05	0.43 ± 0.08	1.31 ± 0.03	0.13 ± 0.01	0.98	
14-Feb-2008	1.74 ± 0.04	0.58 ± 0.10	1.16 ± 0.06	0.22 ± 0.05	0.92	
17-Apr-2008	1.94 ± 0.01	0.63 ± 0.06	1.31 ± 0.05	0.30 ± 0.03	0.98	
24-Apr-2008	1.84 ± 0.01	0.27 ± 0.02	1.57 ± 0.02	0.18 ± 0.04	0.98	
26-Jun-2008	2.00 ± 0.04	0.51 ± 0.06	1.48 ± 0.03	0.36 ± 0.10	0.76	
3-Jul-2008	1.84 ± 0.02	0.64 ± 0.07	1.20 ± 0.05	0.22 ± 0.06	0.78	
10-Jul-2008	1.99 ± 0.16	0.57 ± 0.28	1.42 ± 0.12	0.36 ± 0.04	0.98	

Date	FDOMm(0) (QSU)	PFDOMm (QSU)	RFDOMm (QSU)	k_M (day ⁻¹)	R ²	c)
20-Sep-2007	1.85 ± 0.02	0.79 ± 0.08	2.64 ± 0.05	0.08 ± 0.02	0.86	
27-Sep-2007	1.55 ± 0.06	0.67 ± 0.12	2.22 ± 0.06	0.06 ± 0.02	0.88	
4-Oct-2007	1.21 ± 0.08	0.48 ± 0.10	1.69 ± 0.01	0.06 ± 0.01	0.94	
31-Jan-2008	1.67 ± 0.05	0.47 ± 0.13	2.14 ± 0.09	0.06 ± 0.01	0.96	
7-Feb-2008	2.08 ± 0.02	0.36 ± 0.07	2.43 ± 0.05	0.04 ± 0.01	0.95	
14-Feb-2008	1.59 ± 0.02	0.27 ± 0.05	1.86 ± 0.02	0.04 ± 0.01	0.97	
17-Apr-2008	1.55 ± 0.02	0.45 ± 0.06	2.00 ± 0.04	0.05 ± 0.01	0.94	
24-Apr-2008	2.79 ± 0.06	0.77 ± 0.11	3.55 ± 0.05	0.06 ± 0.01	0.96	
26-Jun-2008	1.84 ± 0.06	0.75 ± 0.09	2.59 ± 0.04	0.08 ± 0.02	0.90	
3-Jul-2008	1.24 ± 0.03	0.48 ± 0.07	1.72 ± 0.04	0.05 ± 0.01	0.97	
10-Jul-2008	1.91 ± 0.02	0.69 ± 0.07	2.60 ± 0.04	0.07 ± 0.01	0.98	

Date	BP(0) ($\mu\text{g C L}^{-1} \text{ day}^{-1}$)	BP(4) ($\mu\text{g C L}^{-1} \text{ day}^{-1}$)	BP(12) ($\mu\text{g C L}^{-1} \text{ day}^{-1}$)	BP(53/70) ($\mu\text{g C L}^{-1} \text{ day}^{-1}$)	d)
20-Sep-2007	2.0 ± 0.2	0.6 ± 0.1	0.4 ± 0.1	0.1 ± 0.1	
27-Sep-2007	0.8 ± 0.2	0.4 ± 0.1	0.3 ± 0.1	0.1 ± 0.1	
4-Oct-2007	0.7 ± 0.2	0.6 ± 0.1	0.4 ± 0.1	0.1 ± 0.1	
31-Jan-2008	0.9 ± 0.1	0.6 ± 0.1	0.1 ± 0.1	0.1 ± 0.1	
7-Feb-2008	0.3 ± 0.1	0.1 ± 0.1	0.1 ± 0.1	0.1 ± 0.1	
14-Feb-2008	0.7 ± 0.1	0.2 ± 0.1	0.1 ± 0.1	0.0 ± 0.1	
17-Apr-2008	0.7 ± 0.1	0.3 ± 0.1	0.3 ± 0.1	0.2 ± 0.2	
24-Apr-2008	0.8 ± 0.1	0.4 ± 0.1	0.3 ± 0.1	0.0 ± 0.1	
26-Jun-2008	1.0 ± 0.1	0.6 ± 0.1	0.3 ± 0.1	0.0 ± 0.1	
3-Jul-2008	1.2 ± 0.1	0.4 ± 0.1	0.2 ± 0.1	0.0 ± 0.1	
10-Jul-2008	1.3 ± 0.1	0.6 ± 0.1	0.1 ± 0.1	0.0 ± 0.0	

Date	O _{2c} (0) ($\mu\text{mol L}^{-1}$)	O _{2c} (53/70) ($\mu\text{mol L}^{-1}$)	BOD ($\mu\text{mol L}^{-1}$)	BOD-BDOC·R _C ($\mu\text{mol L}^{-1}$)	e)
20-Sep-2007	232.7 ± 0.3	202.4 ± 2.0	30 ± 3	-7 ± 11	
27-Sep-2007	236.4 ± 0.1	214.4 ± 0.7	22 ± 1	-1 ± 3	
4-Oct-2007	237.8 ± 0.5	221.0 ± 1.0	17 ± 2	0 ± 8	
31-Jan-2008	255.7 ± 0.4	234.0 ± 1.0	22 ± 2	8 ± 8	
7-Feb-2008	255.2 ± 0.3	232.6 ± 0.8	23 ± 1	11 ± 7	
14-Feb-2008	249.4 ± 0.3	225.5 ± 2.0	24 ± 2	9 ± 8	
17-Apr-2008	251.5 ± 0.1	222.6 ± 2.4	29 ± 3	10 ± 9	
24-Apr-2008	255.9 ± 0.4	230.9 ± 0.6	25 ± 1	8 ± 7	
26-Jun-2008	233.2 ± 0.4	199.8 ± 2.4	33 ± 3	8 ± 10	
3-Jul-2008	238.9 ± 0.4	204.3 ± 0.2	35 ± 1	14 ± 7	
10-Jul-2008	228.6 ± 0.3	194.4 ± 1.5	34 ± 2	8 ± 9	

Table 3. The obtained significant linear regressions between initial (DOC(0)), bioavailable (BDOC) and refractory (RDOC) DOC, absorption coefficient of CDOM (a₃₅₀), initial (FDOMt(0), FDOMm(0) , FDOMa(0) and FDOMc(0)) and refractory (RFDOMt, RFDOMm) protein-like and humic-like fluorescence, rate constants of DOC (k_{DOC}) and FDOMt (k_T). Slope, intercept, and standard error (SE) are values found by Model II regression. R² = coefficient of determination, p = level of significance, n.s. - not significant.

Eq n°	X	Y	Slope (±SE)	Intercept (±SE)	R ²	p
1	BDOC	BFDOMt	0.037 ± 0.009	n.s.	0.61	<0.01
2	BDOC	PFDOMm	0.03 ± 0.01	n.s.	0.50	<0.02
3	FDOMt(0)	BDOC	23 ± 4	-29 ± 6	0.83	<0.0001
4	FDOMt(0)	k _{DOC}	0.29 ± 0.07	-0.3 ± 0.1	0.63	<0.004
5	FDOMt(0)	k _T	0.49 ± 0.07	-0.7 ± 0.1	0.84	<0.0002
6	FDOMa(0)	RDOC	3.7 ± 0.6	54 ± 2	0.80	<0.001
7	FDOMc(0)	RDOC	6 ± 2	56 ± 3	0.43	<0.03
8	FDOMm(0)	RDOC	9 ± 3	52 ± 4	0.46	<0.03
9	Salinity	FDOMa(0)	-0.3 ± 0.1	15 ± 3	0.54	<0.01
10	Salinity	FDOMc(0)	-0.20 ± 0.08	9 ± 2	0.39	<0.05
11	a ₃₅₀	RDOC	36 ± 11	56 ± 3	0.53	<0.02
12	a ₃₅₀	FDOMm(0)	4.2 ± 0.9	n.s.	0.70	<0.002
13	a ₃₅₀	FDOMa(0)	10 ± 2	n.s.	0.67	<0.003
14	a ₃₅₀	FDOMa(0)	6 ± 2	n.s.	0.40	<0.04
15	BP(0)	BDOC	15 ± 2	n.s.	0.82	<0.0002
16	RFDOMt	RFDOMm	4.3 ± 0.8	-3.4 ± 0.9	0.75	<0.0006
17	RFDOMt	FDOMa(0)	8 ± 3	-7 ± 3	0.38	<0.05
18	RFDOMt	FDOMc(0)	4 ± 1	-3 ± 1	0.64	<0.006*

*Data from the 07/02/08 have been omitted to reach significant levels

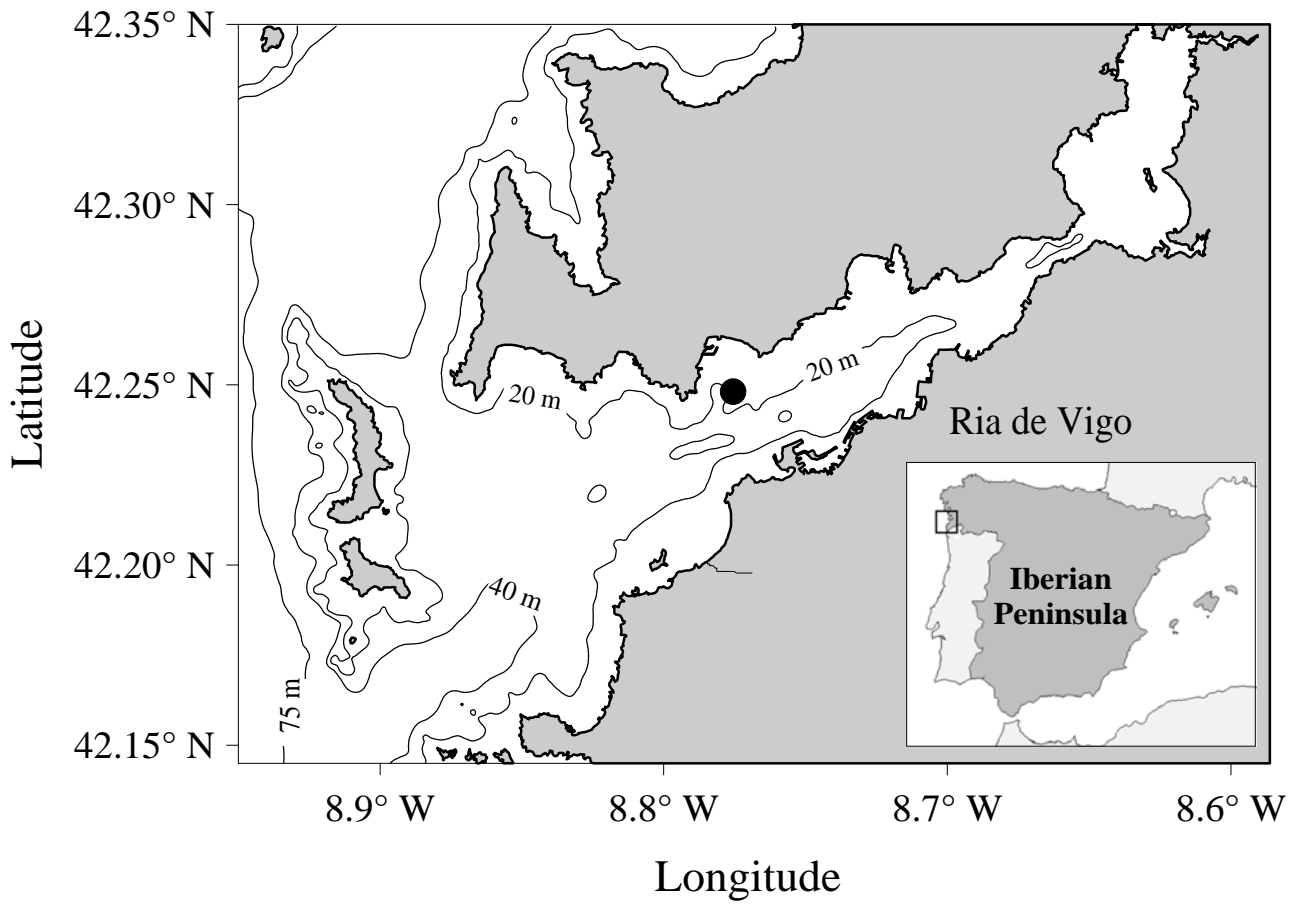


Fig. 1.

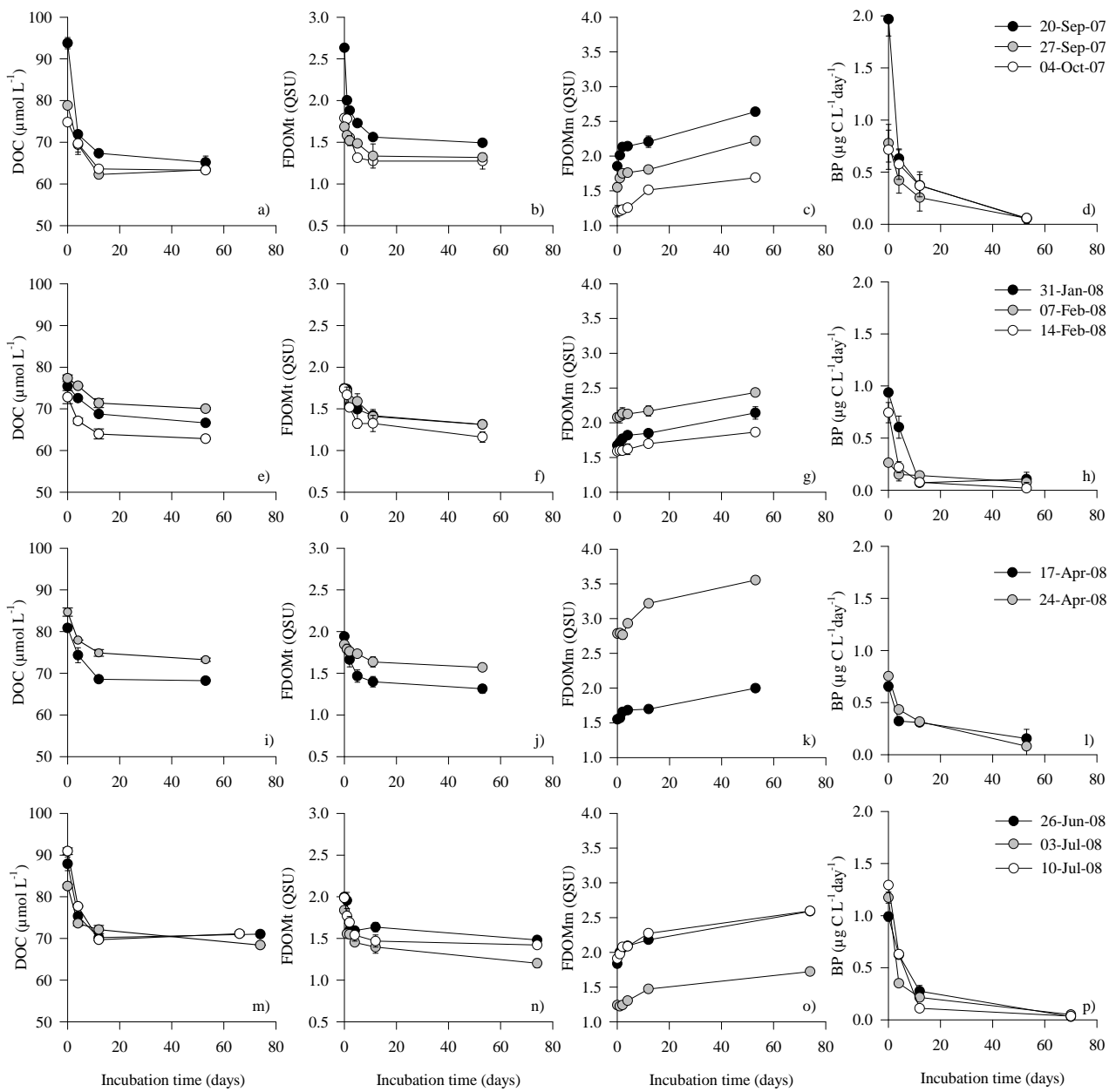


Fig. 2.

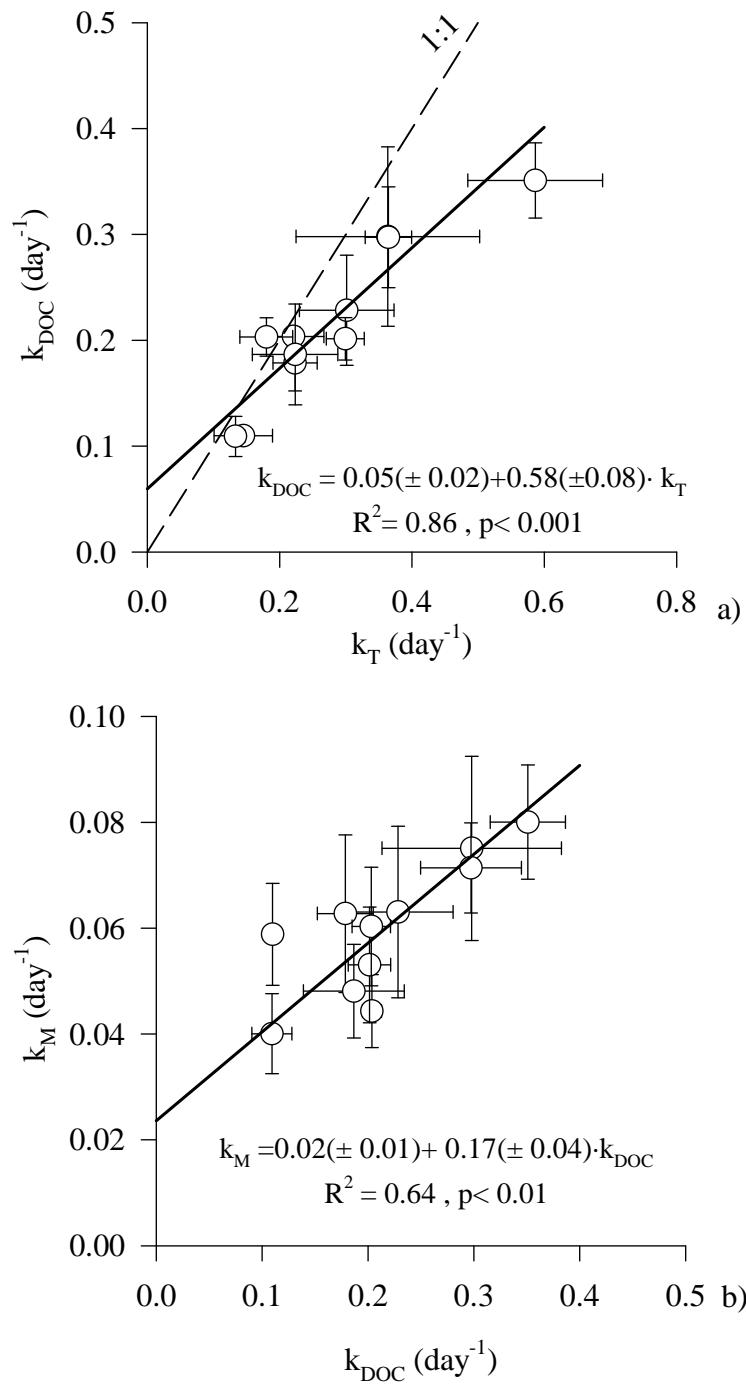


Fig. 3.